3rd International Engineering Conference (IEC 2019)
Federal University of Technology, Minna, Nigeria

Electromagnetic Field analysis of a Single-phase Induction Motor based on Finite Element Method

Omokhafe J. Tola[1], Edwin A. Umoh[2], Enesi A. Yahaya[3], Chika Idoko[4], Ayo Imoru[5]

[1,3,5]Electrical Engineering Department, Federal University of Technology, PMB 65 Minna, Niger State, Nigeria

[2]Electrical Engineering Technology Department, Federal Polytechnic Kaura Namoda, Nigeria

[4]Department of Electrical Engineering, University of Nigeria, Nsukka
*Corresponding author email: enesi.asizehi@futminna.edu.ng, +2348035671462

ABSTRACT
Electric motors are critical components of Electric drives systems, and their performance efficiency has consequences for the fidelity of Electric drives and control. This paper presents an analysis of the electromagnetic field of a single-phase induction motor based on two-dimensional finite element method. The developed model of the machine was used to study its performance characteristics at different speed conditions, a view to affirm the accuracy of the specifications of the motor. The motor losses were analysed and the transient results revealed the losses and a start-up time of 0.07 second with low pulsation at steady state. This implies the specifications are accurate. Therefore, the developed model has possibilities of applications in power system generating systems and industrial plants.

Keywords: Electromagnetic field analysis, finite element analysis, single-phase induction motor, transient analysis.

1 INTRODUCTION

With the recent advances in finite element analysis (FEA), it has become numerically possible to apply finite element method (FEM) to computation of magnetic fields of electrical motors, which is a numerical technique used to determine the distribution of electric or magnetic fields inside a motor, using the solutions of Maxwell's equations.

Single-phase induction motors are generally built in fractional kilowatt size and extensively used in the manufacturing industries for producing power systems and home appliances which rely on electrical rotor actions for their functionalities such as electric fans, refrigerators, vacuum cleaner, air conditioners, pumps, compressors and other types of appliances that may require fractional horsepower (Olarinoye & Oricha, 2013).

Due to the mutual coupling of the two windings (main and auxiliary) and the elliptic electromagnetic field due to the rotor winding in single-phase induction motor air gap, the electromagnetic analysis always poses challenging to designers. Special attention is paid to the machine geometry in the FEA model, by considering the outer and inner diameters of the stator and rotor as well as the air gap length. Compared to analytical method, FEM enables a designer to solve problems that are difficult to consider with analytical method. Since analytical model of any electrical machine cannot represent complex electromagnetic phenomena such as magnetic saturation and skin effect, the use of FEA models take care of these drawbacks. In this paper, the analysis of a single-phase induction motor based on the numerical FEA model is presented. The model was developed with the Electromagnetic Suite (ANSYS MAXWELL), and used to study the performance of the motor. FEA enables a designer to compute the performance characteristics of the motor without the need to physically construct a prototype. The governing mathematical equations are developed to describe the behaviour of the motor. Electromagnetic field occupies a favourable position in engineering sciences and is one of the foundations of electrical engineering. Unlike Finite difference method (FDM), compared to methods such as Boundary element method (BEM) and Moments method (MM), FEM has gained acceptance for solving linear and nonlinear problems without geometrical restrictions (Ramón Bargallo, 2006). Several researchers have applied FEA to analyzed the electromagnetic performance of induction motor (Hong & Hwang, 1991; Williamson, Lim, & Robinson, 1990; Yahiaoui & Bouillault, 1994). In (Belmans et al., 1992),the authors applied FEA to analyzed the magnetic fields of the iron loss in an induction motor. Petkovska and Cvetkovski(Petkovska & Cvetkovski, 2010) used FEM to

analysed the starting characteristics of single phase induction motor by sizing the start-up capacitor.

2 OVERVIEW OF ANYSY MAXWELL'S SIMULATION ENVIRONMENT

ANSYS Maxwell handles low-frequency electromagnetic field simulation. It consists of different solvers, namely electrostatic, magneto-static and transient among others (Tola & Umoh, n.d.). It can be applied to modelling and analysis of electromagnetic and electromechanical devices such as transformers, motors, actuators amongst others. ANSYS uses FEM of solving the Maxwell's equations, and is therefore suitable for a variety of analysis(Maxwell, 2013). The starting point for deriving partial differential equation models for electromagnetic field computations is the application of Maxwell's equations, which relate six sets of vector and scalar: electric field intensity E(V/m), magnetic field intensity H (A/m), electric flux density D (coulomb/m^2), magnetic flux density B (T), electric current density J (A/m^2) and electric charge density ρ (coulomb/m^3) respectively. Therefore, the static reference frame of Maxwell's equations in differential form which governs the equation of the motor are written as follows (.D, n.d.):

$$\begin{cases} \nabla \times E = \dfrac{-\partial B}{\partial t} \\ \nabla \times H = J + \dfrac{\partial D}{\partial t} \\ \nabla \bullet D = \rho \\ \nabla \bullet B = 0 \end{cases} \quad (1)$$

where, E is electric field intensity, D is electric flux density, H is magnetic field intensity, J is electric current density, ρ is electric charge density, B is magnetic field density. The electric field strength is further related by the relationship:

$$J = \sigma E \quad (2)$$

The electromagnetic prodigies defined by Maxwell's equation in static and moving reference frame are expressed as:

$$\begin{cases} B^* = B \\ E^* = E + v \times B \\ H^* = H \\ J^* = J \end{cases} \quad (3)$$

Where the quantities on the right-hand side described the moving reference frame, and the electric field vector E is only quantity modified. The divergence of the magnetic field density is given by:

$$\nabla \bullet B^* = 0 \quad (4)$$

The magnetic vector potential satisfies the following expressions:

$$\nabla \bullet \left(v \nabla A \right) = -J \quad (5)$$

$$J = \sigma E^* = \sigma (E + v \times B) \quad (6)$$

Where$H$ is the magnetic field strength, A is magnetic vector potential, J is the current density, v is the moving velocity, σ is the conductivity of the material.

3 MODEL EQUATIONS OF THE MOTOR

The voltage equation of the (stator)phase winding and rotor bars of the machine are expressed as(Sami Kanerva & Slavomir Seman, n.d.):

$$V_p = \frac{d\psi}{dt} + R_c i + L_e \frac{di}{dt} \quad (7)$$

Where R_c is the resistance of the coils, V_p is the phase voltage and L_e is the coil inductance. The flux linkage of the coils is determined by the relationship:

$$\psi = \sum_{k=1}^{n_c} \beta_k l_k A_k^{ave} \quad (8)$$

Where

β_k is a multiplier l_k is the length of the coil side, A_k^{ave} is the average vector potential.

The currents and the magnetic vector potential are obtained from the field solution (8) where the applied voltages are

source of field to the phase windings in the stator and the rotor.

The electromagnetic torque of the machine expressed as:

$$T_e = l_a \frac{d}{d\theta_r} \int_{\Omega} \int_{0}^{H} B.dHd\Omega \quad (9)$$

Where l_a is the machine axial length, Ω is the cross-sectional area of the air gap and θ_r is the rotor position. The equations governing the movement of the motor are given by:

$$J_m \frac{d\omega}{dt} + B\omega = T_e - T_f \quad (10)$$

$$\frac{d\theta_r}{dt} = \omega \quad (11)$$

Where J_m is the moment of mechanical inertia, B is the damping coefficient, which is very small and can be neglected, ω is the rotational speed, T_e is electromagnetic torque and T_f is the load torque applied externally. FEA analyzes the transient conditions of the motor using two-dimensional vector potential formulation and voltage equations of the windings. Therefore, the field solution is used to determine the magnetic flux density and the magnetic field strength respectively.

Second-order differential equations are used to define the boundary value of two-dimensional finite element analysis. As a result, the magnetic field of the FEM model in two-dimensional plane is analytically expressed as:

$$\frac{\partial A}{\partial x}\left(\frac{1}{\mu}\frac{\partial A}{\partial x}\right) + \frac{\partial A}{\partial y}\left(\frac{1}{\mu}\frac{\partial A}{\partial y}\right) = J - j\omega\sigma A \quad (12)$$

Where ω is the angular frequency of the magnetic field. The development of the FEA model of the single-phase induction motor is based on the procedure established in (Tola & Umoh, n.d.). The geometry dimension, and other parameters used are tabulated in Table I. Based on Eq. (4) to (11), the magnetic vector potential and current density are computed by finite element method using ANSYS Maxwell software.

Table I: Single-phase induction motor parameters.

Parameter	Value
Rated Output Power (kW)	0.37
Number of the stator slot	24
Stator outer diameter (mm)	95
Stator inner diameter (mm)	55.25
Air gap (mm)	0.25
Number of the rotor slot	18
Rotor inner diameter (mm)	16
Stator core length (mm)	65
Rated speed (rpm)	3750

The results obtained and portrayed by Fig. 1 to Fig. 4 showed the performance characteristics of the proposed single-phase induction motor design using ANSYS Maxwell. These results meet the required specifications for the design of the motor.

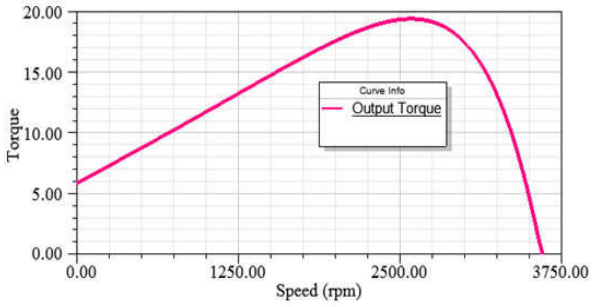

Fig. 1. Torque versus rotor speed

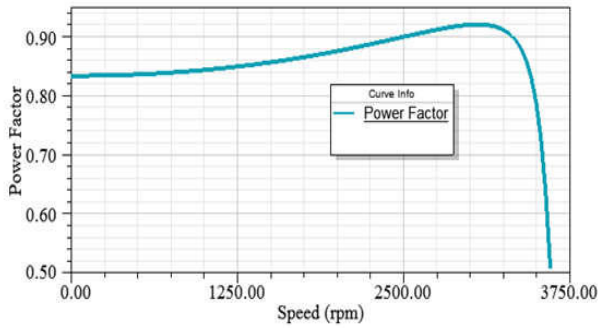

Fig. 2. Power factor versus rotor speed

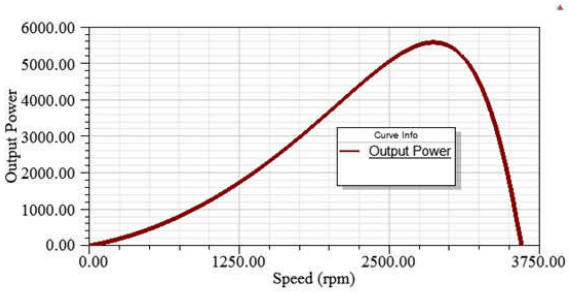

Fig. 3. Output power versus rotor speed

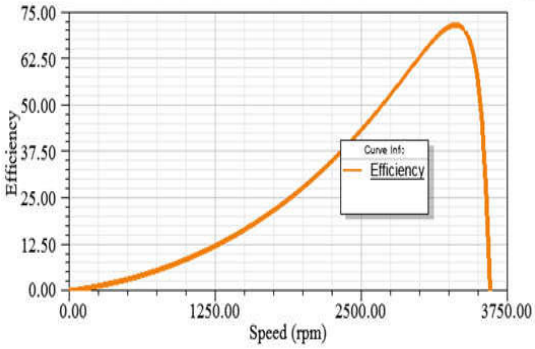

Fig. 4. Efficiency versus rotor speed

A. Meshing

The cross-section of the motor is divided into some two-dimensional elements which determines the accuracy of the magnetic vector potential A. Triangular elements are typically used for 2-D models and each element is related by several nodes by the relationship:

$$\phi^e(x,y) = \sum_{j=1}^{3} N_j^e(x,y)\phi_j^e \qquad (13)$$

Where $N_j^e(x,y)$ are expansion functions which are expressed by the relationship:

$$N_j^e(x,y) = \frac{1}{2\Delta^e}(a_j^e + b_j^e x + c_j^e y)\phi_j^e \qquad (14)$$

Where Δ^e is the area of the e[th] element.Fig. 5 shows the mesh generation of the model, and its spread over the whole cross-section of the motor. Fig. 6 shows the equivalent circuit of the motor.

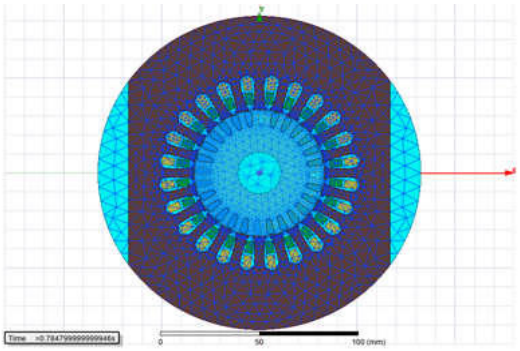

Fig. 5. 2-D mesh of the motor

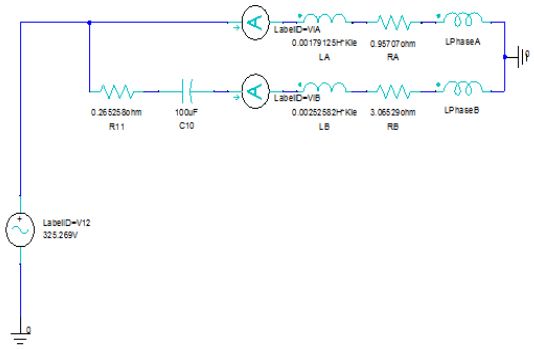

Fig. 6. The equivalent circuit of the motor

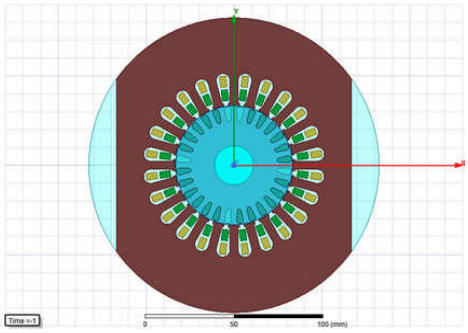

Fig. 7. 2-D model of the motor

3.1 SIMULATION OF RESULTS

The dynamic operation of the induction motor with 100mF capacitor, 230V supply at 50 Hz are analyzedand presented. The dynamic characteristics used in (Krzysztof MAKOWSKI & Marcin J. WILK, 2011)were also used in this study. The transient behavior of the machine was simulated under no-load condition, with stopping time of

2s at 0.002 steps. The starting waveforms of the motor are depicted in Fig. 8 – Fig. 11.

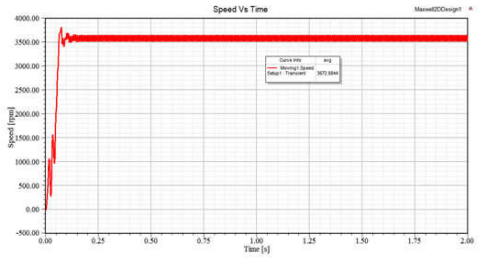

Fig. 8. Rotor speed

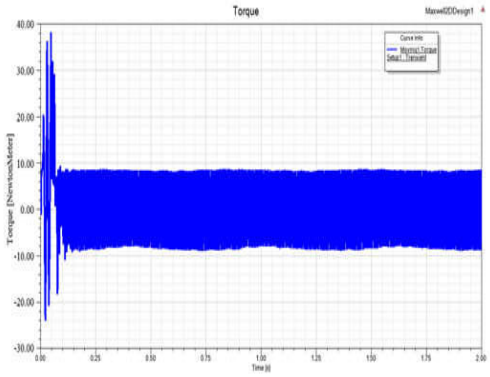

Fig. 9. Electromagnetic Torque

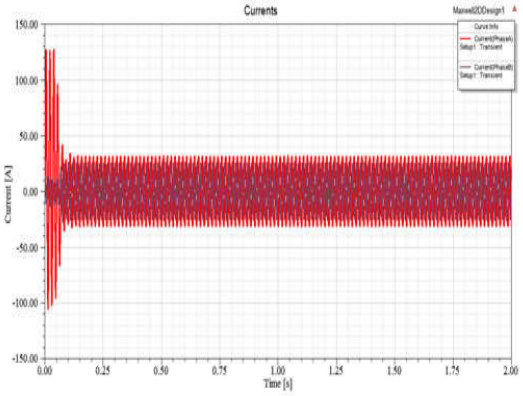

Fig. 10. Stator currents

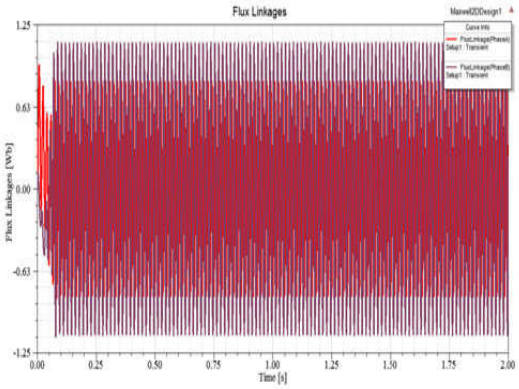

Fig. 11. Flux Linkages

The motor starts and reaches synchronous speed in 0.07 seconds. The elliptical rotational field in the air gap due to the asymmetry of the stator windings leads to non-uniform running of the rotor. It was observed that the capacitor placed on the auxiliary winding increases the start-up of the motor and a phase shift increase.

3.2 ANALYSIS OF LOSSES

The efficiency of a single-phase induction motor can be used to gauge it performance. Electrical engineers have continued to optimize electric motors with the aim of improving their efficiencies. However, a universal challenge during optimization of motor efficiency relates to losses in the magnetic circuit of the motor. Motor losses may be broadly classified as stator copper loss, core losses, rotor eddy current losses and windage loss (Huynh, Zheng, & Acharya, 2009)(Engineering, Ko, Jang, Park, & Lee, 2010). Copper loss includes I^2R loss. Core losses occur when the magnetic material is exposed to a time-varying magnetic flux, and is made up of two major components- hysteresis loss and eddy current loss, and are measured based on sinusoidal flux density of fluctuating magnitude and frequency. It can be expressed as (Gordon, R. Slemon, 1990)(Smith, 1995):

$$P_{Core} = K_h f \hat{B}_{\max}^{\alpha} + K_e f^2 \hat{B}_{\max}^{2} \quad (15)$$

Where f is frequency, $B_{\max}$ is the peak flux density in Tesla,

K_h , K_e and α are constants for the core material.

SOLID LOSS

The stranded loss which is the ohmic loss of multi-turn coils or stranded type coil. it can be determined by the expression(Tikhonova, Malygin, Beraya, Sokolov, & Plastun, n.d.):

$$P = \frac{1}{\sigma}\int_V J^2 dV \qquad (16)$$

Where V is the volume. In research, core loss, solid loss and stranded loss are a major concern. However, hysteresis and eddy-current loss are often neglected in the performance analysis of electrical machines due to the difficulty in the classical formula caused by the distribution of magnetic field strength and flux density. Fig. 12 depicts results associated with the motor. However, with proper selection of the magnetic material, the core loss will be negligible. Fig. 13 and Fig. 14 portrayed the distribution of magnetic line and magnetic flux density on of the 2-D module machine. The presence of high magnetic flux density distribution in the stator and rotor can be lowered by implementing a high-quality material at the critical point of motor construction.

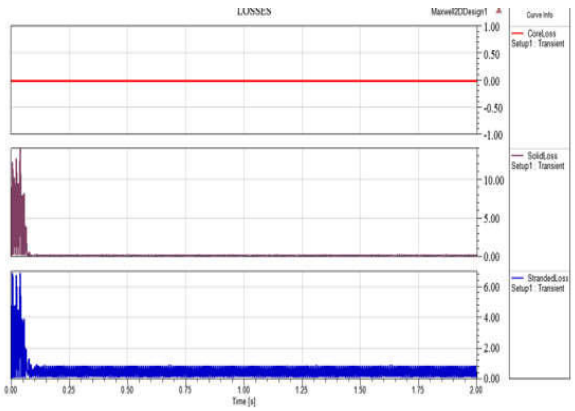

Fig.12:Losses associated with the motor

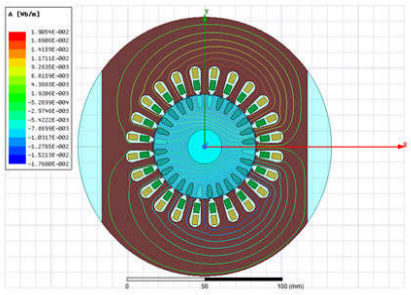

Fig. 13. Magnetic line of flux of the 2-D model motor

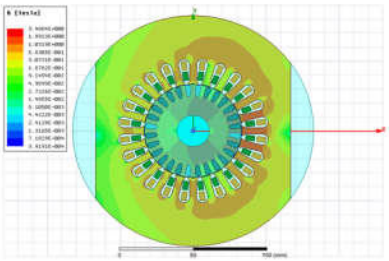

Fig. 14. The magnetic flux density of the 2-D model motor

The divergence *div* of the magnetic flux density, B given in (4) was computed using the ANSYS program. The computed value was *div* B = 4.14E-017 which is approximately equal to zero.

4 CONCLUSION

An analysis of the electromagnetic field of a single-phase induction motor using ANSYS Maxwell was presented. The analysis of the dynamic performance characteristics of the motor shows a good starting torque and a minimal pulsating of the rotor speed. The motor has a short start-up time of 0.07s, but the pulsation at steady state that generates the elliptic rotational field in the air gap due to the asymmetry of the main and auxiliary winding. The losses associated with the motor were clearly shown from the results presented. These results indicate that the modeled motor is a good candidate for industrial applications.

REFERENCE

Belmans, R., Verdyck, D., Geysen, W., Findlay, R. D., Szabados, B., Spenser, S., & Lie, S. (1992). Magnetic Field Analysis in Squirrel Cage Induction Motor. *IEEE Transaction on Magnetic*, *28*(2), 1367–1370.

Ko, K., Jang, S., Park, J., & Lee, S. (2010). *Electromagnetic losses calculation of 5kW class high-speed permanent magnet synchronous motor considering current waveform*. *39*(3), 7062.

Gordon, R. Slemon, X. . (1990). Core Losses in Permanent magnet motors. *IEEE Transactions on Magnetics*, *26*(5).

Hong, C. H., & Hwang, G. J. (1991). Non Linear *Finite Element Modeling for Electrical Energy Applications Lecture Notes for ET4375*.

Belmans, R., Verdyck, D., Geysen, W., Findlay, R. D., Szabados, B., Spenser, S., & Lie, S. (1992). Magnetic Field Analysis in Squirrel Cage Induction Motor. *IEEE Transaction on Magnetic*, *28*(2), 1367–1370.

Ko, K., Jang, S., Park, J., & Lee, S. (2010). *Electromagnetic losses calculation of 5kW class high-speed permanent magnet synchronous motor considering current waveform*. *39*(3), 7062.

Gordon, R. Slemon, X. . (1990). Core Losses in Permanent magnet motors. *IEEE Transactions on Magnetics*, *26*(5).

Hong, C. H., & Hwang, G. J. (1991). Non Linear Complex Finite Element Analysis of Squirrel Cage Induction Motor Performance. *Electrical Power Application Institute of Electrical Engineering Proceeding*, 277–284.

Huynh, C., Zheng, L., & Acharya, D. (2009). *Losses in High Speed Permanent*. *131*(March), 2–7. https://doi.org/10.1115/1.2982151

Krzysztof MAKOWSKI, & Marcin J. WILK. (2011). Determination of dynamic characteristics of the single-phase capacitor induction motor. *Electrotechnical Review Vol 87, No. 5*, 231–237.

Maxwell, A. (2013). *ANSYS Maxwell V16*. 1–31.

Olarinoye, G. A., & Oricha, J. Y. (2013). *A Method for Solving the Voltage and Torque Equations of the Split-Phase Induction Machines*. *10*(1), 1–6.

Petkovska, L., & Cvetkovski, G. (2010). *FEM based assessment of capacitor sizing on starting characteristics of a single-phase induction motor*. (12), 113–116.

Ramón Bargallo. (2006). *Finite Element for Electrical Engineer*. UNIVERSITAT POLITÈCNICA DE CATALUNYA, ELECTRICAL ENGINEERING DEPARTMENT.

Sami Kanerva, & Slavomir Seman. (n.d.). Inductance Model for Coupling Finite Element Analysis With Circuit Simulation. *IEEE Transaction on Magnetic*, *41*(5), 1620–1623.

Smith, K. E. (1995). Influence of manufacturing Processes on Iron losses A.C. *IEEE Conference on Electrical Machine Drive*, (412).

Tikhonova, O., Malygin, I., Beraya, R., Sokolov, N., & Plastun, A. (n.d.). *LOSS CALCULATION OF INDUCTION MOTOR WITH RING WINDINGS BY " ANSYS MAXWELL ."* *5*(11), 63–66.

Tola, O. J., & Umoh, E. A. (n.d.). MODELING AND ANALYSIS OF A PERMANENT MAGNET SYNCHRONOUS GENERATOR DEDICATED TO WIND ENERGY CONVERSION. *2nd International Engineering Conference (IEC 2017) Federal University of Technology, Minna, Nigeria*, 216– 223